

# Fano Resonances in Nanoscale Plasmonic Systems: A Parameter-Free Modeling Approach

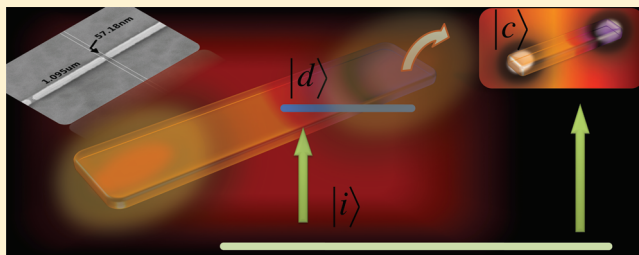
Vincenzo Giannini,\* Yan Francescato, Hemmel Amrania, Chris C. Phillips, and Stefan A. Maier

Department of Physics, Imperial College London, London SW7 2AZ, United Kingdom

**S** Supporting Information

**ABSTRACT:** The interaction between plasmonic resonances, sharp modes, and light in nanoscale plasmonic systems often leads to Fano interference effects. This occurs because the plasmonic excitations are usually spectrally broad and the characteristic narrow asymmetric Fano line-shape results upon interaction with spectrally sharper modes. By considering the plasmonic resonance in the Fano model, as opposed to previous flat continuum approaches, here we show that a simple and exact expression for the line-shape can be found. This allows the role of the width and energy of the plasmonic resonance to be properly understood. As examples, we show how Fano resonances measured on an array of gold nanoantennas covered with PMMA, as well as the hybridization of dark with bright plasmons in nanocavities, are well reproduced with a simple exact formula and without any fitting parameters.

**KEYWORDS:** Fano resonances, plasmonics, localized surface plasmons, plasmon hybridization, nanoantennas, Fano theory



The spectral shaping of plasmon resonances in metal nanostructures via controlled plasmon hybridization and Fano interferences is receiving growing attention, due to the possibility of designing new materials with a controlled response to light at the nanoscale.<sup>1–6</sup> Fano interferences are also involved in the unprecedented signal enhancement occurring when vibrational excitations of a molecule are coupled with a plasmon resonance in surface-enhanced IR absorption (SEIRA) spectroscopy<sup>7</sup> and in many other interactions of plasmonic systems with sharp resonances in atoms, molecules, and quantum dots. More generally, indeed a considerable number of phenomena occurring on the nanoscale are described by the interference of two different excitation pathways. In particular, if in one path a discrete state (DS) is excited and in the other a continuum state (CS), Fano resonances may arise.<sup>8–12</sup> Fano theory hence explains the results obtained in a large number of areas of physics and supplies a simple and powerful tool that allows one to understand deeply several common physical situations. A defining characteristic of these resonances is their asymmetric line profile due to the close coexistence of destructive and constructive interferences.<sup>12</sup> Indeed, when destructive and constructive phenomena take place at close energy positions, very sharp resonances are observed. Fano published his first results in 1935<sup>8</sup> concerning the autoionization of noble gases, and a more general and incisive work appeared in 1961.<sup>9</sup> Majorana arrived at similar conclusions in 1931, working on the role of selection rules for the nonradiative decay of two electronic excitations in atomic spectra;<sup>13,14</sup> in his papers, he considered the interaction between discrete and continuum channels.

Important examples of Fano interferences are found in the ionization of atoms,<sup>8</sup> Raman scattering,<sup>15</sup> molecular spectroscopy,<sup>16,17</sup> quantum transport,<sup>18</sup> optical absorption in quantum wells<sup>19</sup> and light propagation in photonic devices;<sup>20,21</sup>

there is a very rich literature on this topic, partially surveyed in recent reviews by Miroshnichenko, Luk'yanchuk and Nie.<sup>10,12,22</sup> Recently, it has been shown that in plasmonic nanostructures it is also possible to observe this phenomenon.<sup>1–5,7,10,11,23,24</sup> In this case, the excitations are achieved through the interference of a plasmon resonance (PR), which acts as the CS, with a DS. Depending on the situation, the DS can be the electronic excitation of a molecule,<sup>4,7,24</sup> the excitation of a diffraction channel (e.g., gratings, hole arrays, or plasmonic crystals),<sup>25–29</sup> the excitation of a dark plasmon mode<sup>1,2,5</sup> or the excitation of a guided mode.<sup>20</sup> Curiously, the first reported Fano resonance, by Wood in 1902, belongs nowadays to the field of plasmonics.<sup>30</sup> He measured asymmetric resonances studying the light reflection by metallic gratings; however, since at that time no satisfying explanation was found, these were named Wood's anomalies. The first understanding of the profiles was given by Fano, who considered the excitation of surface modes by such a grating.<sup>25</sup> Although Fano resonances have been known for a long time, still there is a need to fill the gap between theory and experimental results obtained when plasmonic resonances are involved. Generally, the approach to study these asymmetric resonances is to fit them with a Fano profile,<sup>23</sup> to apply a scattering matrix method considering all the channels as discrete levels,<sup>20</sup> or by means of classical phenomenological models consisting of coupled oscillators.<sup>31</sup> All these methods can give good results, but, they neither add nor predict any information about the real physical process nor do they answer several questions; for example, (i) How does the energy width of the PR affect the profile? (ii) How does the

**Received:** April 11, 2011

**Revised:** May 25, 2011

**Published:** June 03, 2011

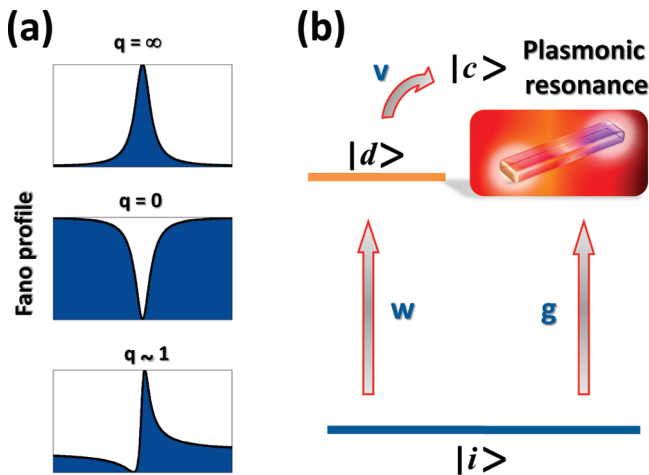


**Figure 1.** (a) Different Fano line-shapes obtained varying the value of the asymmetry parameter  $q$  when the continuum is flat. (b) Fano process with a plasmonic continuum state; an incident state  $|i\rangle$  excites a quasi-continuum state obtained from the interaction of a plasmonic resonance,  $|c\rangle$ , with a discrete state  $|d\rangle$ . The interaction is described by the coupling factors  $w, g$ , and  $v$ .

asymmetry depend on the energy separation between the PR and DS? (iii) Why does the dip in the Fano resonance have a lower energy than the peak or vice versa? (iv) What is the effect of the coupling strength between the DS and PR?

In this Letter, we consider the interaction of a plasmonic resonance (acting as the CS) with a discrete resonance, in the framework of the Fano model<sup>9,32</sup> (see Figure 1). The result is a new mixed state that accounts for both excitation paths. We perform exact calculations of the probability of exciting that mixed state, and we obtain a simple analytic description of Fano resonances mediated by PRs. Remarkably, this formulation enables also the possibility of studying the interaction of DSs with sharp plasmonic resonances. As an example, we compare theory and experiment for the extinction cross section of an array of gold nanoantennas covered with PMMA. The absorption peak of the PMMA at  $1730\text{ cm}^{-1}$  interferes with the localized surface plasmon resonance (LSPR), giving rise to a Fano line-shape. We reproduce these results with a simple formula and without any fitting parameters. As a second example, we apply our theory to an all-plasmonic system sustaining bright and dark plasmon modes.

The shape of the resonance caused by the coupling of a DS with a flat CS has the following form,<sup>9</sup>

$$\sigma(\mathcal{E}) = \frac{(\mathcal{E} + q)^2}{\mathcal{E}^2 + 1} \quad (1)$$

Here  $q$  is the shape parameter that determines the asymmetry of the profile and is expressed as the excitation probability ratio between the discrete and the continuum state.  $\mathcal{E}$  is the reduced energy, which depends on the energy of the incident photons  $E$ , on the energy of the DS,  $E_d$ , and its width,  $\Gamma_d$ ;  $\mathcal{E}$  is defined as  $2(E - E_d)/\Gamma_d$ .<sup>23</sup> Three special cases of the Fano formula 1 are obtained when  $q \rightarrow \infty$ ,  $q = 0$ , and when  $q$  is different from 0 or  $\infty$ . In the first case, the probability of directly exciting the continuum is small and the profile is determined by the transition through the DS; this results in a Lorentzian line-shape (see Figure 1a, top) and describes, for example, the Breit–Wigner resonance common in atomic and nuclear scattering.<sup>10</sup> When  $q = 0$ , a symmetric antiresonance arises, (see Figure 1a, middle) known

as Breit–Wigner dip;<sup>10</sup> when  $q$  is finite, an asymmetric line-shape (see Figure 1a, bottom) is obtained that is typical in many-body systems and known as Feshbach resonance.<sup>10</sup> It has been shown recently that all three Fano resonance cases can be achieved in plasmonics, where the formula 1 is widely used in order to describe these processes.<sup>12</sup>

Note that in eq 1 no feature of the PR is included. Here we overcome this limitation by considering that the coupling to the CS is governed by the excitation of a PR. We first consider the unperturbed Hamiltonian  $\mathcal{H}_0$ , which has a DS  $|d\rangle$ , with eigenvalue  $E_d$ , and a CS  $|c\rangle$ , with a continuum spectra of eigenvalues  $E$ . Following the prediagonalized states method of Fano, we assume that the DS  $|d\rangle$  is coupled to the continuum state  $|c\rangle$  by a coupling Hamiltonian  $V$  (see Figure 1b), and the matrix elements of  $\mathcal{H}_0$  and  $V$  are

$$\langle d|\mathcal{H}_0|d\rangle = E_d = 0 \quad (2a)$$

$$\langle c|\mathcal{H}_0|c'\rangle = E\delta(E - E') \quad (2d)$$

$$\langle c|V|d\rangle = v\sqrt{\mathcal{L}(E)} \quad (2c)$$

where we chose the discrete energy state as the origin, i.e.,  $E_d = 0$ .  $|c\rangle$ ,  $|c'\rangle$  and  $E, E'$  are different states and their respective energies within the continuum. In eq 2c, the coupling of the discrete state to the continuum is given by  $v(\mathcal{L}(E))^{1/2}$ , i.e. it is determined by the plasmonic line-shape  $\mathcal{L}(E)$  and by the coupling factor  $v$ . The plasmonic line-shape  $\mathcal{L}(E)$  is a Lorentzian with energy position  $E_p$  and width  $\Gamma_p$  given by the PR

$$\mathcal{L}(E) = \frac{1}{1 + \left(\frac{E - E_p}{\Gamma_p/2}\right)^2} \quad (3)$$

Also, we assume that all the other matrix elements of  $V$  are zero, that is

$$\langle d|V|d\rangle = \langle c|V|c'\rangle = 0 \quad (4)$$

We first solve the eigenvalue problem  $\mathcal{H}|\Psi\rangle = E|\Psi\rangle$ , where  $\mathcal{H} = \mathcal{H}_0 + V$ , and  $\Psi$  is the new mixed quasi-CS. Second, we consider an incident photon in the DS  $|i\rangle$  that is coupled by the Hamiltonian  $W$  to the states  $|d\rangle$  and  $|c\rangle$  (see Figure 1b)

$$\langle i|W|d\rangle = w \quad (5a)$$

$$\langle i|W|c\rangle = g\sqrt{\mathcal{L}(E)} \quad (5b)$$

where  $w$  and  $g$  are the coupling factors.

The Fano profile is recovered by solving the previous problem (see Supporting Information) and by calculating the probability that a photon in state  $|i\rangle$  excites a quasi-CS  $|\Psi\rangle$ , that is,  $|\langle i|W|\Psi\rangle|^2$ . If we normalize the latter result to the probability of exciting the continuum in the absence of the DS, that is, the PR, the same result of eq 1 is obtained, but now  $q$  and  $\mathcal{E}$  are also linked to the PR as

$$\frac{|\langle i|W|\Psi\rangle|^2}{|\langle i|W|c\rangle|^2} = \frac{(\mathcal{E} + q)^2}{\mathcal{E}^2 + 1} \quad (6a)$$

$$q = \frac{vw/g}{\Gamma_d(E)/2} + \frac{E - E_p}{\Gamma_p/2} \quad (6b)$$

$$\mathcal{E} = \frac{E}{\Gamma_d(E)/2} - \frac{E - E_p}{\Gamma_p/2} \quad (6c)$$

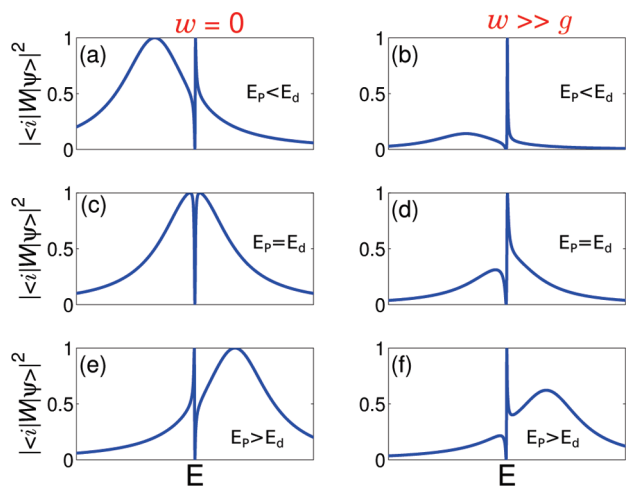


**Figure 2.** Fano resonances calculated from eqs 6a–6c for two different coupling regimes, (a,c,e)  $w = 0$ ; (b,d,f)  $w \gg g$ ; when a DS with energy  $E_d$  interacts with a continuum plasmon state with energy  $E_p$  ( $\Gamma_p = 10\Gamma_d$ ) for different relative positions. (a,b)  $E_p < E_d$ , (c,d)  $E_p = E_d$ , and (e,f)  $E_p > E_d$ .

where  $\Gamma_d(E) = 2\pi\nu^2\mathcal{L}(E)$  is related to the DS energy width. It is simple to see in fact, that  $\Gamma_d(E)$  coincides with the decay rate of the DS when the continuum is flat and when it is possible to apply Fermi's golden rule (i.e.,  $V$  is small compared with  $\mathcal{H}_0$ ), as can be seen from eqs 2c and 3.

Equations 6a–6c describe the interaction of a PR with a discrete state. In this case  $q$  and  $\mathcal{C}$  are no longer constant; they depend on the coupling factors, on the PR width  $\Gamma_p$ , and on the plasmon energy  $E_p$ . This explains why the Fano resonance exhibits different degrees of asymmetry depending on the physical situation.

For example, in Figure 2 we plot the profiles obtained with eqs 6a–6c in the most common situation, that is, when the plasmon width  $\Gamma_p$  is much bigger than  $\Gamma_d$ . Two main cases are considered. In the first, the coupling factor to the DS,  $w$ , is very small compared with the other coupling factors  $\nu$  and  $g$  ( $w = 0$ , see Figure 2 panels a,c,e); in the second case, we consider  $w \gg g$  (see Figure 2 panels b,d,f). Furthermore, we take in account the three possible situations between the plasmon energy and the discrete level, that is,  $E_p < E_d$  (Figure 2a,b),  $E_p = E_d$  (Figure 2c,d) and  $E_p > E_d$  (Figure 2e,f).

When  $w$  is small we see a line-profile that is mainly determined by the plasmon resonance, which is modified by the coupling to the DS. This happens because the DS is being mainly excited indirectly through the plasmonic state (see Figure 1b). Also, it is important to note that the minimum of the Fano resonance always lies between the two maxima arising from the discrete and plasmon states; in the situation  $E_p = E_d$  (Figure 2c) a symmetric dip is obtained.

These kind of resonances are particular to several physical situations, for example, Fano resonances due to the hybridization of dark with bright plasmons<sup>1,2,5</sup> or coupling of molecular vibrational excitations with broadband PRs.<sup>4,7,24</sup> Actually, in all these cases a weak interaction of the incident photons with the DS is present. A similar behavior is found when  $w$  is not zero but still small, except for an asymmetry observed in the case  $E_p = E_d$  (not shown).

We have a different scenario when  $w \gg g$ , that is, when the interaction with the quasi-continuum mainly goes through the DS (see Figure 2b,d,f). In this case, the main resonance is due to

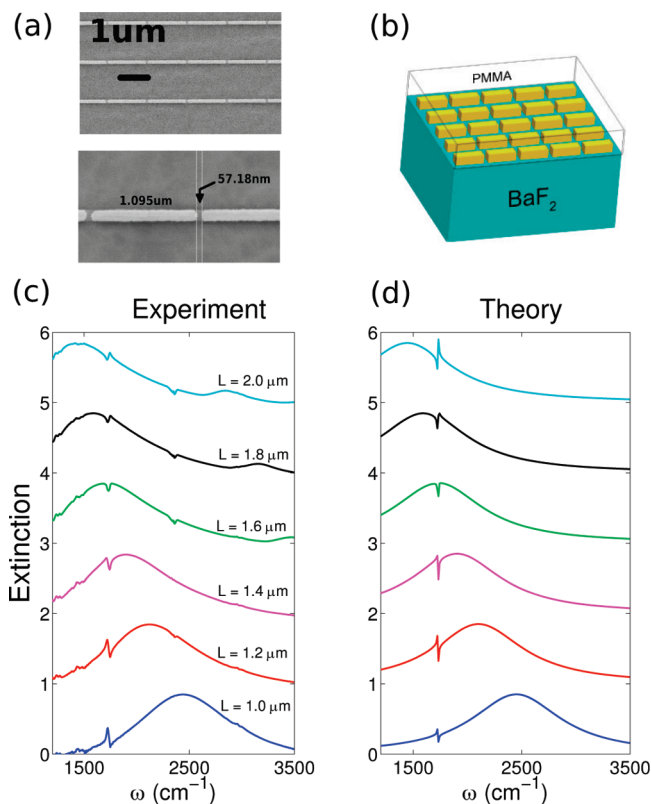


**Figure 3.** (a) Scanning electron microscope top view image of an array of gold nanoantennas. (b) Schematic representation of the array covered with PMMA on a BaF<sub>2</sub> substrate. (c) Measured and (d) calculated (with eqs 6a–6c) extinction of an array of nanoantennas as a function of the frequency  $\omega$  and the nanoantenna length  $L$ . The incident light is polarized parallel to the long axis of the antennas.

the DS, particularly in the cases  $E_p < E_d$  (Figure 2b) and it weakens when the plasmon resonance moves toward higher energies (Figure 2f). Strikingly, now we can see in Figure 2f that the minimum is at lower energy than two maxima. This represents an important difference from Figure 2e that can be helpful in order to understand in which coupling regime we are in. Between the two extreme cases,  $w = 0$  and  $w \gg g$ , fall the phenomena of extraordinary transmission in metallic hole arrays,<sup>26</sup> excitation of PRs in metal gratings,<sup>25</sup> or lattice resonances in plasmonic crystals.<sup>27–29</sup>

We note that this formalism also allows the value of the energy position of the minimum in the Fano resonance, that occurs when  $q = -\mathcal{C}$  (see eqs 6a–6c), to be obtained. From eqs 6a–6c, it is simple to see that the minimum is obtained when  $E = -\nu w/g$  (note that  $w$  has dimensions of an energy, while, due to the continuum normalization, it is  $\nu^2$  and  $g^2$  that have dimensions of an energy). Interestingly, the energy of the minimum position does not depend on the PR, but only on the coupling factors.

Next, we show that eqs 6a–6c are indeed valuable tools for predicting Fano resonances in plasmonic systems without the need for brute-force numerical electromagnetic modeling. Let us consider a PR formed in a Au nanoantenna coupled to a vibrational resonance of an adjacent molecule. Figure 3 shows the tuning of the Fano line-shape via shifting the PR position with respect to this vibrational resonance. The studied system (see Figure 3b) is an array of gold nanoantennas fabricated by e-beam lithography deposited on barium fluoride (BaF<sub>2</sub>) and spincoated

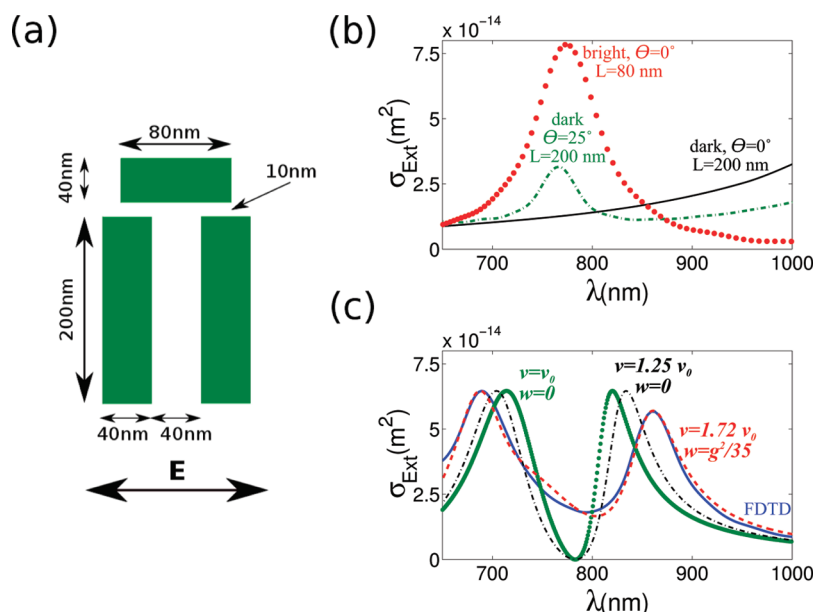


**Figure 4.** (a) Dolmen structure composed of two 200 nm parallel gold antennas close to a 80 nm perpendicular one. The electric field is polarized along the shorter antenna. (b) Extinction cross sections calculated by FDTD for single antennas with dimensions  $80 \times 40 \times 40$  nm and  $200 \times 40 \times 40$  nm; the shorter antenna (dotted red line) presents a dipolar mode close to the dark resonance of the longer antenna (full black and dashed green line with  $0$  and  $25^\circ$  tilt, respectively). (c) Extinction cross sections of the dolmen structure as obtained from FDTD (full blue line) and from eqs 6a–6c with different coupling factors (interrupted lines); completely dark resonance, i.e.,  $w = 0$ , with coupling through near-field similar to bright resonance excitation (i.e.,  $\nu = (\Gamma_d/2\pi)^{1/2} = \nu_0$ , dotted green line) or tuned to show better agreement ( $\nu = 1.25\nu_0$ , dot-dashed black line), small direct excitation of the dark resonance ( $w = g^2/35$  and  $\nu = 1.72\nu_0$ , dashed red line).

with PMMA. The latter exhibits a strong and distinct resonance at  $1730\text{ cm}^{-1}$  arising from the stretching of the C=O bond. The nanoantennas are 20 nm thick, 100 nm wide, and their lengths vary from 1 to 2  $\mu\text{m}$ , spaced laterally by 1.2  $\mu\text{m}$  and separated by 50 nm from each other along their main axis (see Figure 3a,b).

In Figure 3c, we show the measured extinction spectra, that is,  $[1 - \text{transmittance}]$ , of the various samples. Increasing the nanoantennas length, the LSPR is moving from higher to lower energies, crossing the DS due to PMMA absorption. For each curve in Figure 3c, we can clearly see the main resonance corresponding with the LSPR and the asymmetric feature due to the Fano interference. Note that the incident electric field is polarized along the main antennas axis.

These results can be theoretically reproduced by means of eqs 6a–6c. From the experiments it is possible to obtain  $\Gamma_p$  and  $E_p$  (extinction obtained without PMMA), as well as  $\Gamma_d$  and  $E_d$  (from the PMMA absorption). The coupling factor  $g$  is given by the probability of exciting the plasmon resonance with a plane wave, in other words by the plasmon resonance width, that is,  $g^2 \sim \Gamma_p/2\pi$ . Considering that the plasmon resonance is much broader than the PMMA resonance, the coupling factor  $\nu$  is given with a good approximation via Fermi's golden rule, as  $\nu^2 \sim \Gamma_d/2\pi$ , while  $w$  can be obtained by means of the Einstein coefficients, considering that in the experiment we are in the linear regime of low-power excitation, implying  $w \sim \nu$ .<sup>33</sup> Hence, we have all the ingredients for eqs 6a–6c and the result is shown in Figure 3d; we can appreciate a very good agreement without any fitting parameters, while it is very common to use eq 6a and search a constant  $q$  that gives a reasonable fit.

In Figure 3c we can see that the minimum does not reach zero as in Figure 2, this is because in the experiment not all the molecules in the sample are interacting with the nanoantennas, but actually only the molecules present in the gap.<sup>11</sup> Also, the

molecules can decay in different states that are not plasmons or photons (i.e., heat). This results in the presence of a component in the transmitted light that does not interfere.

We now apply our formalism to an all-plasmonic system with interfering bright and dark plasmon modes. We choose a dolmen-type structure<sup>2,34</sup> consisting of a short and two longer gold<sup>35</sup> nanoantennas (see Figure 4a). The long nanoantenna alone has a second-order resonance around  $\lambda = 800$  nm (dashed green line in Figure 4b, extinction cross section), and for symmetry reasons<sup>11</sup> it is possible to excite this resonance only when the incident light is not perpendicular to the antenna, otherwise we have a completely dark resonance (full black line in Figure 4b). The short nanoantenna alone now is of a dimension so that a dipole (first order, bright) resonance is excited almost at the same wavelength as the aforementioned dark resonance (dotted red line in Figure 4b). Now we consider a composite structure with both kinds of nanoantennas arranged in a dolmen configuration as in Figure 4a. The incident field is normal to the structure and polarized along the shorter nanoantenna, that is, only the dipolar resonance can be excited. In Figure 4b, we show the extinction cross section (full blue curve) of that structure, calculated with a finite-difference time-domain method (FDTD). We can see that the interaction of the dark and bright mode results in a Fano resonance.<sup>2,34</sup> Note that the incident field cannot excite the dark resonance directly, but only through the dipolar resonance which, via near-field coupling, excites the dark mode. The Fano interference can now be studied with our model, where the dark mode plays the role of the discrete state. In order to do so we assume that the coupling factor between an incident photon and the dark mode,  $w$ , is zero and the coupling to the dipolar plasmon resonance is  $g^2 \sim \Gamma_p/2\pi$ . The widths  $\Gamma_p$  and  $\Gamma_d$  are obtained from the plasmonic resonances (Figure 4b). The last parameter required is the coupling factor  $\nu$  between the dark and the dipolar

mode. Clearly this parameter depends on the details of the geometry, particularly the distance between the antennas, and therefore should be obtained by a detailed study varying these parameters. In a first attempt, we will simply assume a behavior similar to the bright resonance, that is,  $\nu^2 \sim \Gamma_d/2\pi$ . The result is shown in Figure 4c (dotted green line); even though the approximation is rough we can see an overall shape that is very close to the FDTD simulation. Therefore our theoretical model allows us to quickly and quite accurately predict the main features of the observed spectral response in the coupled system.

A further improvement is possible by tuning the unknown parameter  $\nu$ ; this is shown in Figure 4c (dot-dashed black line,  $\nu = 1.25(\Gamma_d/2\pi)^{1/2} = 1.25\nu_0$ ). Now the resonances are more separated and move toward the result obtained by FDTD. However, there are still some discrepancies in the minimum position and in the strength of the second resonance.

The minima does not reach zero in the FDTD simulation due to the photons absorbed in the structures during the Fano interference. As in the previous case (Figure 3), the “lost” photons can be considered as an additive background term in the eq 6a. Also, note that the slight strength difference of the two resonances can be taken into account if  $w$  differs from zero, that is, the dark resonance is not completely dark due to the asymmetry of the dolmen nanostructure. Following these considerations, we can see in Figure 4c (dashed red line) that a very good agreement is reached when  $\nu = 1.72\nu_0$  and  $w = g^2/35$ . Note also that  $w$  is very small compared with the other coupling constants, as expected being the discrete state a dark resonance.

It is important to remark that the previous example shows that when the width of the two resonances are comparable the Fano model describes plasmon hybridization theory.<sup>36</sup> This means that an analytical description of plasmon hybridization model is provided by our theory as well. Lastly, note that it is now possible to obtain the width and position of the noninteracting bright and dark resonances from the measured experimental Fano interference spectrum.

In conclusion, we have shown that considering a plasmonic resonance in the Fano model a simple and exact analytic relation can be found. This allows the role of the plasmonic mode in the Fano interference to be understood in a way that properly takes into account the width and the position of the plasmonic resonance and of the sharp mode. The description is general and can also describe the case where the resonances have similar widths, that is, not just when the continuum state is much broader than the discrete one. This theory is particularly useful for understanding experimental results in plasmonics.

We have demonstrated that through the coupling factors to the discrete or to the continuum state a full description of many situations where a Fano resonance can be observed in plasmonics is obtained, particularly for the interaction of bright modes with dark modes or for the interaction of emitters with nanoantennas. Important additional examples include the extraordinary transmission of light in hole arrays and the lattice resonances in plasmonic crystals. The theory outlined in this work now allows a quick and parameter-free prediction of Fano interferences in such systems.

## ■ ASSOCIATED CONTENT

Supporting Information. Additional information provided. This material is available free of charge via the Internet at <http://pubs.acs.org>.

## ■ AUTHOR INFORMATION

### Corresponding Author

\*E-mail: [v.giannini@imperial.ac.uk](mailto:v.giannini@imperial.ac.uk).

## ■ ACKNOWLEDGMENT

This work was sponsored by the Engineering and Physical Sciences Research Council (EPSRC) and from Leverhulme Trust. V.G. acknowledges funding from the EU through the Marie Curie IEF program. Thanks to Hong Yoon for the PMMA spincoating, Dr. Rob Airey for the sample fabrication, and Ana O’Loughlen for the stimulating discussions.

## ■ REFERENCES

- (1) Hao, F.; Sonnefraud, Y.; Van Dorpe, P.; Maier, S. A.; Halas, N. J.; Nordlander, P. *Nano Lett.* **2008**, *8*, 3983–3988.
- (2) Verellen, N.; Sonnefraud, Y.; Sobhani, H.; Hao, F.; Moshchalkov, V. V.; Van Dorpe, P.; Nordlander, P.; Maier, S. A. *Nano Lett.* **2009**, *9*, 1663–1667.
- (3) Fan, J. A.; Wu, C.; Bao, K.; Bao, J.; Bardhan, R.; Halas, N. J.; Manoharan, V. N.; Nordlander, P.; Shvets, G.; Capasso, R. *Science* **2010**, *328*, 1135–1138.
- (4) Pryce, I. M.; Aydin, K.; Kelaita, Y. A.; Briggs, R. M.; Atwater, H. A. *Nano Lett.* **2010**, *10*, 4222–4227.
- (5) Sonnefraud, Y.; Verellen, N.; Sobhani, H.; Vandenbosch, G.; Moshchalkov, V.; Van Dorpe, P.; Nordlander, P.; Maier, S. *ACS Nano* **2010**, *4*, 1664–1670.
- (6) Lassiter, J. B.; Sobhani, H.; Fan, J. A.; Kundu, J.; Capasso, F.; Nordlander, P.; Halas, N. J. *Nano Lett.* **2010**, *10*, 3184–3189.
- (7) Neubrech, F.; Pucci, A.; Cornelius, T. W.; Karim, S.; García-Etxarri, A.; Aizpurua, J. *Phys. Rev. Lett.* **2008**, *101*, 157403.
- (8) Fano, U. *Nuovo Cimento* **1935**, *12*, 154–161.
- (9) Fano, U. *Phys. Rev.* **1961**, *124*, 1866–1878.
- (10) Miroshnichenko, A.; Flach, S.; Kivshar, Y. *Rev. Mod. Phys.* **2010**, *82*, 2257–2298.
- (11) Giannini, V.; Fernández-Domínguez, A. I.; Sonnefraud, Y.; Roschuk, T.; Fernández-García, R.; Maier, S. A. *Small* **2010**, *6*, 2498–507.
- (12) Luk’yanchuk, B.; Zheludev, N. I.; Maier, S. A.; Halas, N. J.; Nordlander, P.; Giessen, H.; Chong, C. T. *Nat. Mater.* **2010**, *9*, 707–715.
- (13) Majorana, E. *Nuovo Cimento* **1931**, *8*, 78–83.
- (14) Majorana, E. *Nuovo Cimento* **1931**, *8*, 107–113.
- (15) Rousseau, D. L.; Porto, S. P. S. *Phys. Rev. Lett.* **1968**, *20*, 1354–1357.
- (16) Nitzan, A.; Jortner, J. *Mol. Phys.* **1972**, *24*, 109.
- (17) Nunes, L. A. O.; Ioriatti, L.; Florez, L. T.; Harbison, J. P. *Phys. Rev. B* **1993**, *47*, 13011–13014.
- (18) Kohler, S.; Lehmann, J.; Hänggi, P. *Phys. Rep.* **2005**, *406*, 379–443.
- (19) Aleshkin, V. Y.; Antonov, A. V.; Gavrilenko, L. V.; Gavrilenko, V. I. *Phys. Rev. B* **2007**, *75*, 125201.
- (20) Christ, A.; Tikhodeev, S. G.; Gippius, N. A.; Kuhl, J.; Giessen, H. *Phys. Rev. Lett.* **2003**, *91*, 183901.
- (21) Aizpurua, J.; Taubner, T.; de Abajo, F. J. G.; Brehm, M.; Hillenbrand, R. *Opt. Express* **2008**, *16*, 1529–1545.
- (22) Nie, Z.; Petukhova, A.; Kumacheva, E. *Nat. Nanotechnol.* **2010**, *5*, 15–25.
- (23) Genet, C.; van Exter, M. P.; Woerdman, J. P. *Opt. Commun.* **2003**, *225*, 331–336.
- (24) Neubrech, F.; Weber, D.; Enders, D.; Nagao, T.; Pucci, A. *J. Phys. Chem. C* **2010**, *114*, 7299–7301.
- (25) Fano, U. *J. Opt. Soc. Am.* **1941**, *31*, 213–222.
- (26) Ebbesen, T. W.; Lezec, H. J.; Ghaemi, H. F.; Thio, T.; Wolff, P. A. *Nature* **1998**, *391*, 667–669.
- (27) Auguie, B.; Barnes, W. L. *Phys. Rev. Lett.* **2008**, *101*, 143902.

- (28) Vecchi, G.; Giannini, V.; Gómez Rivas, J. *Phys. Rev. Lett.* **2009**, *102*, 146807.
- (29) Giannini, V.; Vecchi, G.; Gómez Rivas, J. *Phys. Rev. Lett.* **2010**, *105*, 266801.
- (30) Wood, R. W. *Philos. Mag.* **1902**, *4*, 396.
- (31) Klein, M. W.; Tritschler, T.; Wegener, M.; Linden, S. *Phys. Rev. B* **2005**, *72*, 115113.
- (32) Cohen-Tannoudji, C.; Dupont-Roc, J.; Grynberg, G. *Atom-Photon Interactions: Basic Processes and Applications*; John Wiley and Sons, Inc.: New York, 1998.
- (33) Loudon, R. *The Quantum Theory of Light*; Oxford University Press: New York, 1973.
- (34) Zhang, S.; Genov, D. A.; Wang, Y.; Liu, M.; Zhang, X. *Phys. Rev. Lett.* **2008**, *101*, 047401.
- (35) Lynch, D. W.; Hunter, W R. *Handbook of optical constants of solids*; Academic Press: New York, 1985.
- (36) Prodan, E.; Radloff, C.; Halas, N.; Nordlander, P. *Science* **2003**, *302*, 419–422.